Green synthesis of silver nanoparticles using a combination of *Urtica dioica* and *Scrophularia striata* plant extracts and evaluation of their antifungal effects against dermatophytes

Mahtab Bolon[1], *Khosrow Chehri[1], Sajad Moradi[2] and Mohsen Shahlaei[2]

[1]Department of Biology, Faculty of Sciences, Razi University, Kermanshah, Iran
[2]Nano Drug Delivery Research Center, Health Technology Institute, Kermanshah University of Medical Sciences, Kermanshah, Iran
[*]Corresponding author's email: khchehri@gmail.com

Abstract

Infection of the skin is caused by various microbial agents such as fungi. Given the alarming spread of microbial resistance, a new therapeutic approach to combat antibiotic-resistant microbes such as nanoparticles seems necessary. The objective of this study was the investigation of properties of silver nanoparticles synthesized by a mixed extract of *Scrophularia striata* and *Urtica dioica* and to evaluate their biological activity against skin infectious fungi. ultra violet (UV) spectroscopy, dynamic light scattering (DLS), X-ray diffraction (XRD), Fourier transform infrared spectroscopy (FTIR), Energy-Dispersive X-ray (EDAX) and scanning electron microscopy (SEM) were used for characterizing the synthesized nanoparticles. Antimicrobial activity of the nanoparticles was then evaluated against three dermatophytes namely *Microsporum canis*, *Trichophyton rubrum* and *Candida albicans* by measuring the growth disc diameter method. Minimum inhibitory concentration (MIC) and minimum fungicidal concentration (MFC) were also determined using microdilution technique. The maximum absorption peak of the nanoparticles was observed at 450 nm, which is in the range of absorption for silver nanoparticles. X-ray diffraction also confirmed the presence of nano silver crystals. The electron microscopy imaging showed that the nanoparticles were spherical in shape and have an average size of 40±5 nm. MIC value for biosynthesized nanoparticles were 31, 15 and 7 ppm for *T. rubrum*, *M. canis* and *C. albicans*, respectively. It is suggested that the silver nanoparticles synthesized by using a combination of *U. dioica* and *S. striata* extracts could be used as potent antifungal agents against the skin-deep pathogenic fungi.
Keywords: Antifungal effect, Green synthesis, *Scrophularia striata*, Silver nanoparticles, *Urtica dioica*.

Introduction

Dermatophytes are the most important and common fungal pathogens that keratinize the skin, each of which has its own symptoms and different treatment options (Bar *et al.*, 2009). The most important genera of keratinophilic agents include *Microsporum*, *Trichophyton*, *Epidermophyton*, which are abundant in soil and can infected humans (Majid *et al.*, 2015). Over the past few decades, the rate of emergence of new antifungal resistant strains has been higher than the development rate of new antibiotics. This trend has the major economic and health impacts on human societies. Therefore, there is an emergence for developing the new effective agents and methods for the management of fungal infections. The use of nanotechnology in medicine, has already shown its tremendous impact in the pharmaceutical industries (Pereira and Tagkopoulos, 2019). So far, many researches have conducted research on nanoparticles and their antimicrobial properties (Girón-Vázquez *et al.*, 2019; Li *et al.*, 2020; Um-e-Aiman, 2021). The use of organisms such as plants in the biosynthesis of nanoparticles as a new method with less toxicity and risk is one of the most widely used methods that have advantages over chemical and physical methods such as compatibility with the environment, no need for temperature, pressure, energy, as well as use for the production of nanoparticles on a large scale. Nanoparticles due to their special properties show higher inhibitory effect at lower concentrations than antibiotics (Wei *et al.*, 2015; Hernández-Díaz *et al.*, 2021).

Urtica dioica and *Scrophularia striata* are herbaceous perennial plant in the family Urticaceae and Scrophulariaceae, respectively, which have long been used by humans for their healing properties. Gallic acid, formic acid, carotene and vitamin A, tannin, mucilage and vitamin C are the major chemical compounds of *U. dioica*, but the *S. striata* chemical constituents have not been identified yet (Farzami *et al.*, 2004; Matin *et al.*, 2019).

In recent years, researchers have found that by increasing the surface-to-volume ratio of silver metal nanoparticles, their physical and chemical properties can be altered that enhance in their ability to kill fungi and bacteria (Zhang *et al.*, 2019). The objective of this study was the investigation of properties of silver nanoparticles synthesized by a mixed extract of *U. dioica* and *S. striata* and to

evaluate their antifungal activity against skin infectious fungi.

Materials and Methods

Procurement of materials

The *U. dioica* and *S. striata* plants used in this study were prepared from local markets (Kermanshah, Iran) and were powdered by electric milling. Potato dextrose agar (PDA) and potato dextrose broth (PDB) culture media were purchased from Merck (Germany), $AgNO_3$ and fluconazole from Sigma and fungal samples were prepared from Iranian Research Organization for Science and Technology (IROST).

Preparation of aqueous extract

Five grams of plant powder per were poured into 100 mL of distilled water and boiled for 10 minutes. The extracts were then filtered using Whatman paper it was then centrifuged at 10000 rpm for 10 min and the precipitate was discarded. The supernatant was finally transferred through a syringe filter 0.22 µm to eliminate contaminations and then stored at 4 °C.

Green synthesis of silver nanoparticles

Ten milliliters of combined extract containing 7 mL of *S. striata* and 3 mL of *U. dioica* extract (2 mg mL^{-1}) were added to 90 mL of silver nitrate solution (1 mM). The solution was exposed to sunlight for 15 min till the color of solution changed from the yellow to brown confirming the synthesis of silver nanoparticles. The reaction solution was centrifuged at 10,000 rpm for 15 min. The precipitate was washed with deionized water for 3 times in order to complete elimination of unreacted materials.

Characterization of silver nanoparticles

Synthesized AgNPs were first characterized by UV-Vis spectroscopy. The UV-Vis spectroscopy was carried out by using a single beam spectrophotometer (Agilent-Germany) and the spectra was recorded from 200 to 800 nm. The FTIR analysis was carried out by using a Burker instrumentation. The morphology of NPs was determined by FE-SEM, Zeiss Sigma, Model 8100. Size distribution of the SpNPs was measured using Malvern Zetasizer Ultra based on DLS method. The XRD analysis was carried out by using a Bruker Vantec-500 area detector (Cu Ka; l = 1.5418 Å).

Antifungal assay

Candida albicans ATCC 10231 (PTCC5027), *T. rubrum* PTCC 5143 (R613) and *M. canis* PTCC 5069 were used for the antifungal studies. Fungal lyophilized pellets were cultured on potato dextrose agar plates according to the user's manual instructions.

Agar dilution methods

Potato dextrose agar (PDA) was completely mixed with different concentrations of nanoparticles. After 24 h, 50 µL of the standard McFarland from each fungus was spread on the culture medium and incubated at 28 °C 48 h for *C. albicans* and one week for *M. canis* and *T. rubrum* due to slow growth. The tests were repeated three times for each fungus.

Minimum inhibitory concentration

Four rows of 96 well microplates were considered for each fungus and 100 µL of PDB was added to each cell. 100 µL of nanoparticles (500 ppm) was poured into the first well and continued as a decreasing concentration until the well 7. For the MIC test, the half-McFarland standard for each fungus was used. Then, 10 microliters of freshly prepared fungal species were added to all the cells of the first three rows. Well No. 8 of each row contained only culture medium and fungi were considered as positive control. Fungal suspensions were not added to the fourth row and included different concentrations of nanoparticles and culture medium, which was considered as a negative control. Finally, the initial uptake of all cells was measured by ELISA at 630 nm the microplate was transferred to an incubator at 28 °C after one week, cell uptake was re-measured and compared before and after uptake. A well with the same primary and secondary uptake was selected as the minimum inhibitory concentration. Then two wells before and two wells after MIC were cultured on agar medium and the minimum concentration of nanoparticles in which no growth was observed was determined as the minimum lethal concentration.

Inhibition of fungal disc growth

Dilution agar with mixing method was used. First, different concentrations of nanoparticles were prepared. It was poured into Petri and mixed with PDA in ratio 1: 2 and it was mixed well so that the dispersion of the nanoparticles was uniform across the medium. The nanoparticle environment was exposed for 24 hours at room temperature to detect any contamination. Thereafter, a 6 mm-diameter disc loop was created on the original plate containing the fungus. To inoculate the fungus in the culture medium, the loop was first sterilized on the flame and after cooling the loop, the fungus disk was added to the culture center in the vicinity of the flame and placed in complete contact with the nanoparticle environment. After the fungal mycelium of the control plate (no nanoparticles) reached the wall, growth rate of fungal colony in other petri with ruler measured and recorded the test was repeated three times for each fungus. In this test, negative control (culture medium and fungus) and positive control (fluconazole antibiotic and culture medium) were used. SPSS software was used to analyze microbial

data**.**

Results and Discussion

Dermatophytosis and candidiasis are one of the most important opportunistic fungal diseases in humans (de Oliveira *et al.,* 2019). Today, one of the main difficulties in the treatment of patients with fungal infections is the development of resistance to antifungal drugs, as well as increasing the incidence of fungal infections and the use of various antifungal drugs. Therefore, new measures and treatment methods must be adopted (Jansen *et al.,* 2066; Jafarzadeh *et al.,* 2017). In this study the silver nanoparticles were synthesized using mixed plant extract of *U. dioica* and *S. striata* and the resultant was then tested for its antifungal activity against dermatophytes. The antibacterial properties of *U. dioica* and *S. striata* extracts have been reported individually in previously studies (Modarresi-Chahardehi *et al.,* 2012; Zangeneh *et al.,* 2017), but their antifungal activity was reputed for the first time in this study. Also, silver nanoparticles have been synthesized separately by *U. dioica and S. striata* extract and their antibacterial properties have been confirmed (Hatamnia *et al.,* 2020; Abdel-Mageed *et al.,* 2021). However, silver nanoparticles have not been synthesized by combining the extracts of two plants, *U. dioica* and *S. striata*, and the antifungal properties of these nanoparticles have not been studied so far.

In this study the discoloration observed to dark brown in the combination of *U. dioica* and *S. striata* extract was a clear sign of the formation of silver nanoparticles in the reaction (Fig. 1). This color change confirms the reduction of silver metal cations and the synthesis of silver nanoparticles, which is attributed to the cumulative oscillations of free electrons on the metal surface induced by an electromagnetic (Tsuji *et al.,* 2003; Shankar *et al.,* 2004).

In metal nanoparticles, surface plasmon resonance is responsible for their unique optical properties. The fully recorded UV-Vis spectrum indicates an increase in surface plasmon vibrations at a wavelength of 450 nm (Oberdörster *et al.,* 2005). Surface plasmon is the excitation of cumulative charge oscillations at the joint of metal and dielectric. When the frequency of the light that strikes the metal nanoparticles was equal to the frequency of the surface plasmon, the resonance of the surface plasmon occured (Gardea-Torresdey *et al.,* 2002; Oberdörster *et al.,* 2005). Our results show that the maximum wavelength is about 450 nm, which is in agreement with the results of other researchers (Fig. 2).

The results of DLS method showed that the mean hydrodynamic diameter of nanoparticles is around 70 nm with a poly dispersity index (PDI) of 0.25 which indicating the uniformity in the sizes of nanoparticles. This uniformity in size guarantees the stability of nano systems by preventing their flocculation.

In this study, the determination of the X-ray diffraction characteristics has been performed from 10 to 80 degrees using XRD analysis. The peaks at 2 theta 38, 46, 64 and 77 refer to the plans (111), (200), (220) and (311) in the silver crystalline nanoparticles. XRD analysis also shows that silver nanoparticles are synthesized with high purity (Fig. 3). This is concluded from the absence of additional peaks in the XRD pattern. Our results are in line with the findings of other researchers (Sökmen *et al.,* 2004; Mohamed *et al.,* 2019).

Analysis of FTIR spectra showed that the biomolecules in the extract covered the silver nanoparticles as capping agent. A broad band between 3417-3551 cm^{-1} is due to the N–H stretching vibration of NH_2 and OH functional groups related to *U. dioica* and *S. striata* extract molecules. The band at 1637 cm^{-1} corresponds to C=O stretching and peak at 1618 cm^{-1} belongs to NH_2, peak at 1384 cm^{-1} for C-H or CH_3 and aromatic groups. Also peak at 1072 cm^{-1} corresponds to C-O-C, 802 cm^{-1} corresponds to PO and 617 cm^{-1} corresponds to N-H (Fig. 4). Therefore, it can be concluded that some of the water-soluble poly hydroxy compounds such as alkaloids, flavonoids and polysaccharides are present as capping agent in the structure of nano particles, which are in line with the results of other researchers (Emeka *et al.,* 2014; Chandirika and Annadurai, 2018; Kwon *et al.,* 2020).

Scanning electron microscopy (SEM) is a useful tool for studying the surfaces of nano structures and understanding their morphology. The synthesized silver nanoparticles had spherical shape and the mean particle size was determined as 40±5 nm (Fig. 5). The SEM results were in agreement with that of DLS. It should be noted that the presence of some differences in their values are related to the difference in the measurement method. The DLS measures hydrodynamic diameter and hence the obtained results are somewhat larger than the actual size observed in SEM. The result is consistent with the results of other researchers (Bindhu and Umadevi, 2013; Chandirika and Annadurai, 2018).

Elemental analysis of synthesized silver nanoparticles was carried out using EDX technique (Fig. 6) As can be seen, in addition to silver metal as the major component in the nanoparticle structure, other elements such as oxygen, carbon, nitrogen and sulfur are also existed in lesser amounts. This also confirms the result of FTIR analysis which indicated proper coating of silver NPs by organic plant compounds that guarantees good colloidal stability of nano system, which are related to the coating molecules, are less present. These findings are in agreemen with the results of other researchers (Negm *et al.,* 2015; Fatema *et al.,* 2019).

One-way analysis of variance (ANOVA) was

used to analyze the data obtained from antifungal assays. The results of one-way variance between *C. albicans, T. rubrum* and *M. canis* in different concentrations of silver nanoparticles showed that there are significant differences between different groups. To check out the average of which group is different from the rest, Scheffe post hoc test was used and the results are given in Tables 2 to 6. According to Table 1, *C. albicans* and *T. rubrum* did not show any growth up to 31.25 ppm of silver nanoparticles and *M. canis* did not grow up to 62.5 silver nanoparticles. This indicates that the synthesized silver nanoparticles had antifungal properties. As shown in Tables 2 to 6, silver nanoparticles have a significant inhibitory and lethal effect on fungi. The impact of nanoparticles is directly related to the concentration of silver nanoparticles. The higher the concentration of silver nanoparticles, the greater the degree of inhibition so that at a concentration of 500 ppm, the growth of fungi is 100% prevented and even at 7.8 ppm, which is the lowest concentration of nanoparticles, some growth inhibition has been observed which indicates the high antifungal properties of biosynthesized silver nanoparticles (Table 5).

In order to determine the MIC and MFC of silver nanoparticles, 96 well microplates were used for three fungal samples of *C. albicans, T. rubrum* and *M. canis*. The difference between the primary and secondary adsorption of the wells was calculated and the adsorption rates of different concentrations of silver nanoparticles for the three fungal samples are reported in Table 2. By examining the microdilution results, the MIC for *C. albicans* was 7.8 ppm and the MFC was 15.7 ppm. For *T. rubrum* the MIC value was 31.25 ppm and the MFC value was 62.5. The MIC and MFC values for *M. canis* were 15.7 and 31.25, respectively.

Effect inhibition silver nanoparticles biosynthesis in the combined extract of *U. dioica* and *S. striata* on the growth *C. albicans, T. rubrum* and *M. canis* were placed on PDA medium containing concentrations of 500, 250 125, 62.5, 31.25, 15.7, 7.8 ppm of the nanoparticles of silver under study (Figure 7, Table 4). The results are indicative of the effect of synthesized nanoparticles on the growth of fungal mycelium.

Percentage of inhibition of fungal disc growth showed that at a concentration of 500 ppm, 100% of the growth of *C. albicans, T. rubrum,* and *M. canis* was inhibited. The lowest level of inhibition of all mentioned species growth was observed at a concentration of 7.8 ppm with 50%, 40.42%, and 35% inhibition rat for *C. albicans, T. rubrum,* and *M. canis*, respectively (Table 5).

Silver nanoparticles had a greater inhibitory effect on *C. albicans* and this fungus was inhibited at concentrations lower than silver nanoparticles also, less MIC and MFC have been reported for it. *T. rubrum* was more resistant to silver nanoparticles than the other two fungi. The tested extracts have intrinsic antifungal properties, but according to the results, the antifungal properties of biosynthesized silver nanoparticles are higher than the combination of the two extracts and this is due to the special properties of silver and nanoparticles the results of statistical analyzes in Tables 2 to 6 indicate a significant difference between the groups of *C. albicans, T. rubrum* and *M. canis*. Our results demonstrated previously studies (Mousavi *et al.,* 2015; Robles-Martínez *et al.,* 2019; Fatema *et al.,* 2019). Mousavi *et al.* (2015) investigated the antifungal effect of silver nanoparticles with an average diameter of 4 nm on several dermatophyte fungi and reported the MIC level for *M. canis* 200 ppm and stated that this fungus was more resistant than other fungi tested. However, in the present study, the MIC was 15.7 ppm, which is contrary to the results of Mousavi's research and shows that *M. canis* is not very resistant to biosynthesized nanoparticles with a combination of *U. dioica* and *S. striata* extract and at concentrations lower than silver nanoparticles, fungal growth was inhibited. In 2019, Robles Martínez *et al.* (2019) synthesized 26 ± 7 nm silver nanoparticles from garlic extract, tested its antimicrobial activity on *T. rubrum*, and reported growth inhibition at 80 ppm. In the present study, the rate of growth inhibition was reported at a concentration of 31.25 ppm, which indicates that the biosynthesized nanoparticles in this study are stronger.

Conclusion

In this study, aqueous extracts of *U. dioica* and *S. striata* were prepared and 70% *S. striata* and 30% *U. dioica* were mixed to prepare green silver nanoparticles. After changing the color of the solution from pale yellow to brown, UV-Vis absorption of the solution at a wavelength of 450 nm confirmed the synthesis of nanoparticles. The physicochemical characterization of the produced nanoparticles was performed using DLS, FTIR, SEM and XRD analyzes. Altogether the results indicated that the obtained 40 nm size nano particles are capped and stabilized by plant compounds. The antifungal properties of silver nanoparticles produced on three fungi *C. albicans, T. rubrum* and *M. canis* at different concentrations of silver nanoparticles (7.8, 15.7, 31, 25, 62, 52, 125, 250, 500 ppm) were investigated. MIC values for *C. albicans, T. rubrum* and *M. canis* were 7.8, 31.25 and 15.7 ppm, respectively. The results of this study show that the nanoparticles produced from the combination of *U. dioica* and *S. striata* extract have significant antifungal properties *in vitro*. According to the results of this study, it is suggested that the synthesized silver nanoparticles can be used as a suitable antifungal agent against dermatophytes.

Author's contributions

KC conceived and designed research. MB conducted experiments, analyzed data, and wrote the manuscript. All authors read and approved the manuscript. All studies were performed under the supervision of KC and MS.

Conflict of interests

The authors declare that there is no conflict of interest.

Table 1: The result of agar dilution by mixing method.

Extract	Fluconazole	Concentration (ppm)								Fungal species
		0	7.8	15.7	31.25	62.5	125	250	500	
+	-	+	+	+	-	-	-	-	-	*Candida albicans*
+	-	+	+	+	-	-	-	-	-	*Trichophyton rubrum*
+	-	+	+	+	+	-	-	-	-	*Microsporum canis*

+: Growth, -: No growth

Table 2: Mean and standard deviation of microdilution results for tested microorganisms at different concentrations.

Microorganisms	Silver nanoparticles concentration (ppm)	*X* ± SD	F	P
Candida albicans	0	0.2570 ± .00001b-h		
	7.8	0.0780 ± .00283ac-h		
	15.7	-0.0210 ± .00141abd-h		
	31.25	-0.0645 ± .00212a-ce-h	1.106	0.0001
	62.5	-0.0805 ± .00071a-dgh		
	125	-0.0845 ± .00212a-dh		
	250	-0.0910 ± .00141a-e		
	500	-0.0955 ± .00071a-f		
Trichophyton rubrum	0	0.0890 ± .00566b-h		
	7.8	0.0475 ± .00071ad-h		
	15.7	0.0425 ± .00354ad-h		
	31.25	0.0120 ±.00283a-ce-h	616.249	0.0001
	62.5	-0.0025 ± .00071a-dgh		
	125	-0.0115 ± .00212a-dgh		
	250	-0.0405 ± .00071a-fh		
	500	-0.0615 ± .00212a-g		
Microsporum canis	0	0.1560 ± .00001bc-h		
	7.8	0.0395 ± .00071ac-h		
	15.7	0.0815± .00212abdefgh		
	31.25	-0.0430 ± .00141a-h	9.937	0.0001
	62.5	-0.0560 ± .00141a-df-h		
	125	-0.0805 ± .00071a-eh		
	250	-0.0805 ±.00141a-eh		
	500	-0.0920 ± .00141a-h		

(a, b, c, d, e, f, g, h: Show a significant difference. a: compared with concentration 0, b: compared with concentration 7.8, c: compared with concentration 15.7, d: compared with concentration 31.25, e: compared with concentration 62.5, f: compared with concentration125, g: compared with concentration 250, h: compared with concentration 500).

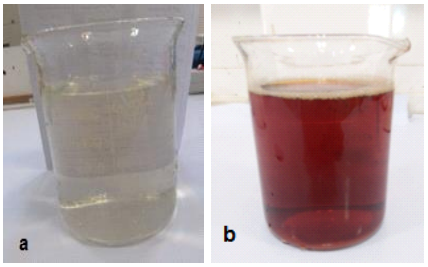

Fig. 1: The process of reducing Ag^{+} to AgNPs. (**a**) Color change before reduction and (**b**) After reduction.

Table 3: Comparison of mean adsorption of different concentrations of silver nanoparticles in three fungi *Candida albicans*, *Trichophyton rubrum* and *Microsporum canis.*

Silver Nanoparticles concentration(ppm)	Group	*X* ± *SD*	F	P
0	**C**	0.2600 ±.00001^{bc}		
	T	0.0850 ± .00707^{ac}	1.341	0.0001
	M	0.1600 ± .00001^{ab}		
7.8	**C**	0.0800 ± .00001^{bc}		
	T	0.0500 ± .00001^{ac}	275.167	0.0001
	M	0.0400 ± .00001^{ab}		
15.7	**C**	-0.0200 ± .00001^{bc}		
	T	0.0400 ± .00001^{ac}	845.237	0.0001
	M	0.0800 ± .00001^{ab}		
31.25	**C**	-0.0650 ± .00707^{bc}		
	T	0.0100± .00001^{ac}	644.103	0.0001
	M	-0.0400 ± .00001^{ab}		
62.5	**C**	-0.0800 ± .00001^{bc}		
	T	-0.0025 ± .00071^{ac}	3.182	0.0001
	M	-0.0600 ± .00001^{ab}		
125	**C**	-0.4450 ± .50205^{b}		
	T	-0.0100 ± .00001^{ac}	1.064	0.0001
	M	-0.0800 ± .00001^{b}		
250	**C**	-0.0900 ± .00001^{bc}		
	T	-0.0400 ± .00001^{ac}	1.015	0.0001
	M	-0.0850 ± .00707^{ab}		
500	**C**	-0.1000 ± .00001		
	T	-0.0600 ± .00001	264.840	0.004
	M	-0.0900± .00001		

C: *Candida albicans*, **T:** *Trichophyton rubrum*, **M:** *Microsporum canis.* a**:** Compared with *Candida albicans*, b: Compared with *Trichophyton rubrum*, c: Compared with *Microsporum canis.* Different letters show a significant difference among the treatments.

Table 4: Mean and standard deviation of measurement of Inhibition of fungal disc growth results for tested microorganisms at different concentrations.

Group	Silver Nanoparticles concentration (ppm)	*X* ± *SD*	F	P
Candida albicans	0	70 ±.00001^{bc_j}		
	7.8	25±.00001^{ad_j}		
	15.7	23.5 ±.70711^{ad_j}		
	31.25	19.5 ±.70711^{a_ce_j}		
	62.5	13 ±1.41421^{a_df_j}		
	125	34.5±.70711^{a_eh_j}	2.423	0.0001
	250	6.5 ±.70711^{a_eh_j}		
	500	.00 ±.00001^{a_j}		
	Fluconazole	.00 ±.00001^{a_j}		
	Extract	62.5 ±.70711^{a_h}		
Trycophyton rubrum	0	70±.00001^{b_j}		
	7.8	41±1.41421^{ad_j}		
	15.7	37.5±.70711^{ae_j}		
	31.25	35±.00001^{abe_j}		
	62.5	16.5±.70711^{a_j}		
	125	10.5±.70711^{a_eg_j}	2.464	0.0001
	250	6.5±.70711^{a_j}		
	500	.00±.00001^{a_h}		
	Fluconazole	.00 ±.00001^{a_gj}		
	Extract	63.5±.70711^{a_i}		
Microsporum canis	0	70±.00001^{b_j}		
	7.8	45.5±.70711^{ac_j}		

	15.7	40.5±.70711^{abe_j}		
	31.25	37.5±.70711^{abf_j}		
	62.5	34.5±.70711^{a_cf_j}		
	125	29.5±.70711^{a_j}	2.328	0.0001
	250	14.5±.70711^{a_j}		
	500	.00±.00001^{a_gj}		
	Fluconazole	.00±.00001^{a_gj}		
	Extract	65±.70711^{a_i}		

(a, b, c, d, e, f, g, h, i, j: Show a significant difference. a: compared with concentration 0, b: compared with concentration7.8, c: compared with concentration 15.7, d: compared with concentration 31.25, e: compared with concentration 62.5, f: compared with concentration125, g: compared with concentration 250, h: compared with concentration 500, i: compared with Fluconazole, j: compared with extract).
Percentage of inhibition of fungal disc growth was obtained using Formula 1: Inhibition rate (%) formula 1,
R: radius of control fungus, r: sample growth radius)

Table 5: Percentage of inhibition of fungal disc growth using Formula 1.

Group	Silver Nanoparticles concentration(ppm)	Inhibition rate (%)
Candida albicans	0	0
	7.8	50
	15.7	66.42
	31.25	72.12
	62.5	81.42
	125	87.85
	250	90.71
	500	100
	Fluconazole	100
	Extract	11.42
Trycophyton rubrum	0	0
	7.8	40.42
	15.7	46.42
	31.25	50
	62.5	76.42
	125	85
	250	90.71
	500	100
	Fluconazole	100
	Extract	10
Microsporum canis	0	0
	7.8	35
	15.7	42.14
	31.25	46.42
	62.5	50.71
	125	58.85
	250	79.28
	500	100
	Fluconazole	100
	Extract	7.14

Table 6: Comparison of mean fungal disc diameter growth at different concentrations of silver nanoparticles for three fungi *Candida albicans, Trichophyton rubrum* and *Microsporum canis.*

Silver Nanoparticles concentration(ppm)	Group	$X \pm SD$	F	P
0	**C**	70 ±.00001		
	T	70 ±.00001	.	.
	M	70 ±.00001		
7.8	**C**	25±.00001^{bc}		

	T	41±1.41421[ac]	278.600	0.0001
	M	45.5±.70711[ab]		
15.7	**C**	23.5 ±.70711[bc]		
	T	37.5±.70711[a]	329.333	0.0001
	M	40.5±.70711[a]		
31.25	**C**	19.5 ±.70711[bc]		
	T	35±.00001[a]	570.500	0.0001
	M	37.5±.70711[a]		
62.5	**C**	13 ±1.41421[c]		
	T	16.5±.70711[c]	266.167	0.0001
	M	34.5±.70711[ab]		
125	**C**	34.5±.70711[c]		
	T	10.5±.70711[c]	537.333	0.0001
	M	29.5±.70711[ab]		
250	**C**	6.5 ±.70711[c]		
	T	6.5±.70711[c]	85.333	0.002
	M	14.5±.70711[ab]		
500	**C**	.00 ±.00001		
	T	.00 ±.00001	.	.
	M	.00 ±.00001		
Fluconazole	**C**	.00 ±.00001	.	.
	T	.00 ±.00001		
	M	.00 ±.00001		
Extract	**C**	62.5 ±.70711		
	T	63.5±.70711	3.167	0.182
	M	65±.70711		

C: *Candida albicans*, **T:** *Trichophyton rubrum*, **M:** Microsporum canis. (a: Compared with *Candida albicans*, b: Compared with *Trichophyton rubrum*, c: Compared with *Microsporum canis*). (a, b, c: Show a significant difference).

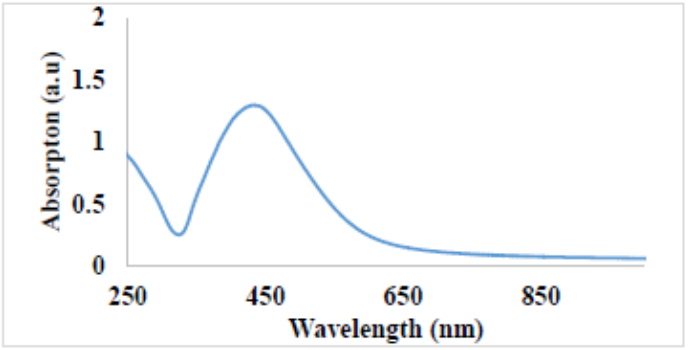

Fig. 2: Absorption spectrum of colloidal silver nanoparticles versus wavelength.

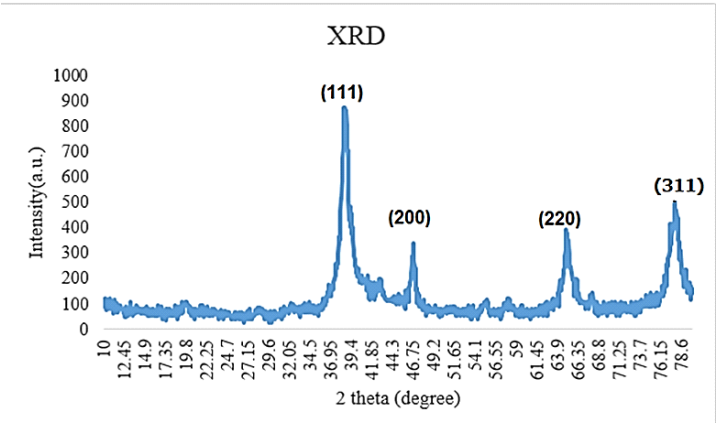

Fig. 3: X-ray diffraction pattern of synthesized silver nanoparticles using a combined of *Urtica dioica* and *Scrophularia striata.*

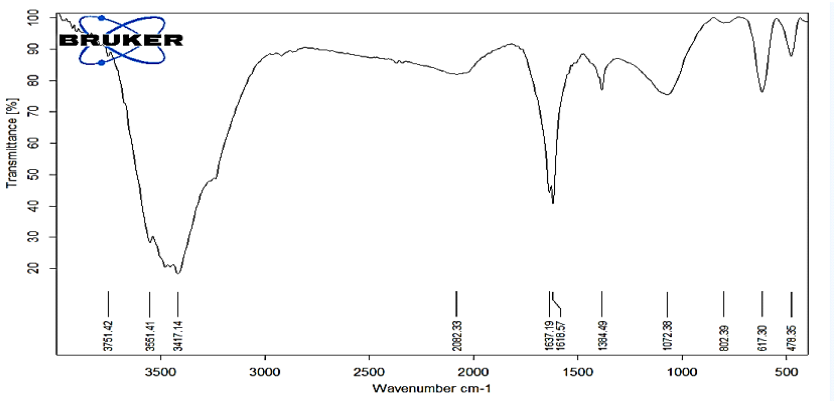

Fig. 4: Fourier transform infrared FTIR spectroscopy of biosynthesized silver nanoparticles using a combined extract of *Urtica dioica* and *Scrophularia striata.*

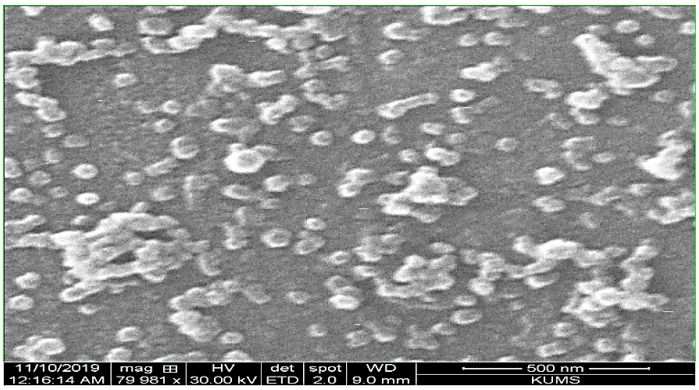

Fig. 5: Scanning electron microscope image (SEM) of biosynthesized silver nanoparticles using a combined extract of *Urtica dioica* and *Scrophularia striata.*

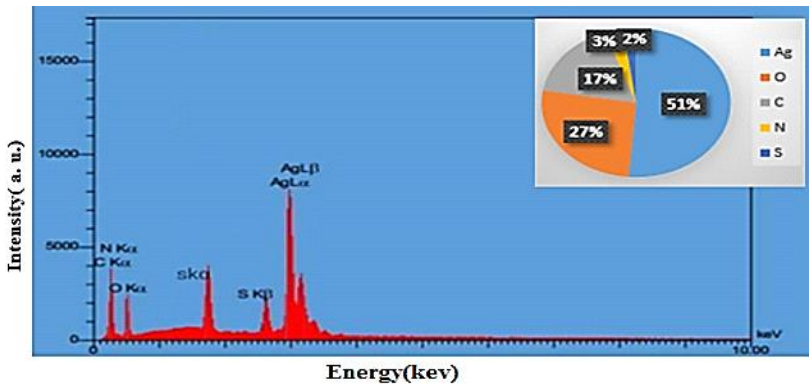

Fig. 6: EDX form of biosynthesized silver nanoparticles using a combined extract of *Urtica dioica* and *Scrophularia striata.*

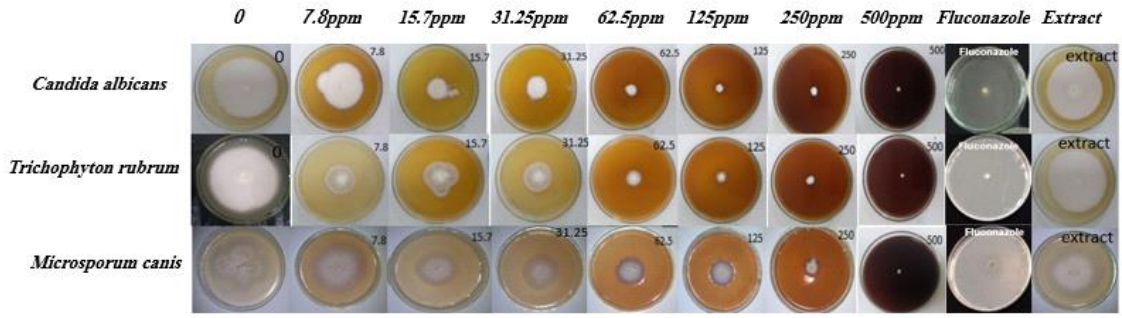

Fig. 7: Fungal growth on PDA medium in the presence of different concentrations of silver nanoparticles.

References

Abdel-Mageed HM, AbuelEzz NZ, Radwan RA, Mohamed SA, 2021. Nanoparticles in nanomedicine: A comprehensive updated review on current status, challenges, and emerging opportunities. *J. Microencapsul*., **38**: 414-436.

Bar H, Bhui DK, Sahoo GP, Sarkar P, Pyne S, Misra A, 2009. Green synthesis of silver nanoparticles using seed extract of *Jatropha curcas*. *Colloids Surf. A Physicochem. Eng. Asp.*, **348**: 212-216.

Bindhu M, Umadevi M, 2013. Synthesis of monodispersed silver nanoparticles using Hibiscus cannabinus leaf extract and its antimicrobial activity. *Spectrochim Acta A Mol. Biomol*., **101**: 184-190.

Chandirika JU, Annadurai G, 2018. Biosynthesis and characterization of silver nanoparticles using leaf extract Abutilon indicum. *Glob. J. Biotechnol. Biochem*., **13**: 7-11.

de Oliveira DBC, Silva LB, da Silva BV, Borges TC, Marques BC, dos Santos MB, 2019. A new acridone with antifungal properties against *Candida* spp. and dermatophytes, and antibiofilm activity against *Candida albicans*. *J. Appl. Microbiol*., **127**: 1362-1372.

Emeka EE, Ojiefoh OC, Aleruchi C, Hassan LA, Christiana OM, Rebecca M, 2014. Evaluation of antibacterial activities of silver nanoparticles green-synthesized using pineapple leaf (*Ananas comosus*). *Micron*, **57**: 1-5.

Farzami B, Ahmadvand D, Vardasbi S, Majin FJ, Khaghan S, 2003. Induction of insulin secretion by a component of *Urtica dioica* leave extract in perfused islets of Langerhans and their *in vivo* effects in normal and streptozotocin diabetic rats. *J. Ethnopharmacol.*, **89**: 47-53.

Fatema S, Shirsat M, Farooqui M, Pathan MA, 2019. Biosynthesis of Silver nanoparticle using aqueous extract of *Saraca asoca* leaves, its characterization and antimicrobial activity. *Int. J. Nano Dimens*., **10**: 163-168.

Gardea-Torresdey J, Parsons J, Gomez E, Peralta-Videa J, Troiani H, Santiago P, 2002. Formation and growth of Au nanoparticles inside live alfalfa plants. *Nano Lett.*, **2**: 397-401.

Girón-Vázquez N, Gómez-Gutiérrez C, Soto-Robles C, Nava O, Lugo-Medina E, Castrejón-Sánchez V, 2019. Study of the effect of *Persea americana* seed in the green synthesis of silver nanoparticles and their antimicrobial properties. *Results Phys*., **13**: 102-142.

Hatamnia AA, Tolouietabar H, Sahraei R, Soheyli E, 2020. Biologically Green synthesis of high-quality silver nanoparticles using *Scrophularia striata* plant extract and verifying their antibacterial activities. *J. Nanostruc*., **10**: 44-51.

Hernández-Díaz JA, Garza-García JJ, Zamudio-Ojeda A, León-Morales JM, López-Velázquez JC, García-Morales S, 2021. Plant-mediated synthesis of nanoparticles and their antimicrobial activity against phytopathogens. *J. Sci. Food Agric*., **101**: 1270-1287.

Jafarzadeh M, Salouti M, Shokri R, 2017. Antifungal activity of silver nanoparticles, copper nanoparticles, their combination and with amphotericin B against *Candida glabrata in vitro* and *in vivo*. *J. Arak Univ. Med. Sci*., 2**0**: 12-21.

Jansen W, Van der Bruggen J, Verhoef J, Fluit A, 2006. Bacterial resistance: a sensitive issue: complexity of the challenge and containment strategy in Europe. *Drug Resist. Updat*., **9**: 123-133.

Kwon H-S, Ryu MH, Carlsten C, 2020. Ultrafine particles: unique physicochemical properties relevant to health and disease. *Exp. Mol. Med*., **52**: 318-328.

Li P, Liang J, Su D, Huang Y, Pan J, Peng M, 2020. Green and efficient biosynthesis of pectin-based copper nanoparticles and their antimicrobial activities. *Bioproc. Biosyst. Eng*., **43**: 2017-2026.

Majid AH, Zahran Z, Rahim AHA, Ismail NA, Rahman WA, Zubairi KSM, 2015. Morphological and molecular characterization of fungus isolated from tropical bed bugs in Northern Peninsular Malaysia, *Cimex hemipterus* (Hemiptera: Cimicidae). *Asian Pac. J. Trop. Biomed*., **5**: 707-713.

Matin T, Ghasemi N, Ghodrati K, Ramezani M, 2019. Green synthesis and characterization of silver nanoparticles using *Scrophularia striata* extract. *Iran. Chem. Commun*., **7**: 594-606.

Modarresi-Chahardehi A, Ibrahim D, Fariza-Sulaiman S, Mousavi L, 2012. Screening antimicrobial activity of various extracts of *Urtica dioica*. *Rev. Biol. Trop*., **60**: 1567-1576.

Mohamed HEA, Afridi S, Khalil AT, Zia D, Iqbal J, Ullah I, et al, 2019. Biosynthesis of silver nanoparticles from *Hyphaene thebaica* fruits and their in vitro pharmacognostic potential. *Mater. Res. Express*., **6**: 1050c9.

Mousavi SAA, Salari S, Hadizadeh S, 2015. Evaluation of antifungal effect of silver nanoparticles against *Microsporum canis, Trichophyton mentagrophytes* and *Microsporum gypseum*. *Iran. J. Biotechnol*., **13**: 38.

Negm NA, Tawfik SM, Abd-Elaal AA, 2015. Synthesis, characterization and biological activity of colloidal silver nanoparticles

stabilized by gemini anionic surfactants. *J. Ind. Eng. Chem*., **21**: 1051-1057.

Oberdörster G, Maynard A, Donaldson K, Castranova V, Fitzpatrick J, Ausman K, 2005. Principles for characterizing the potential human health effects from exposure to nanomaterials: elements of a screening strategy. *Part. Fibre Toxicol*., **2**: 8.

Pereira BMP, Tagkopoulos I, 2019. Benzalkonium chlorides: Uses, regulatory status, and microbial resistance. *Appl. Environ. Microbiol*., **85**: e00377-19.

Robles-Martínez M, González JFC, Pérez-Vázquez FJ, Montejano-Carrizales JM, Pérez E, Patiño-Herrera R, 2019. Antimycotic activity potentiation of *Allium sativum* extract and silver nanoparticles against *Trichophyton rubrum*. *Chem. Biodivers*., **16**: e1800525.

Shankar SS, Rai A, Ahmad A, Sastry M, 2004. Rapid synthesis of Au, Ag, and bimetallic Au core–Ag shell nanoparticles using Neem (*Azadirachta indica*) leaf broth. *J. Colloid Interface Sci*., **275**: 496-502.

Sökmen M, Serkedjieva J, Daferera D, Gulluce M, Polissiou M, Tepe B, 2004. *In vitro* antioxidant, antimicrobial, and antiviral activities of the essential oil and various extracts from herbal parts and callus cultures of *Origanum acutidens*. *J. Agric. Food Chem.*, **52**: 3309-3312.

Tsuji T, Kakita T, Tsuji M, 2003. Preparation of nano-size particles of silver with femtosecond laser ablation in water. *Appl. Surf. Sci*., **206**: 314-320.

Um-e-Aiman, Nisar N, Tsuzuki T, Lowe A, Rossiter JT, Javaid A, Powell G, Waseem R, Al-Mijalli SH, Iqbal M, 2021. Chitin nanofibers trigger membrane bound defence signalling and induce elicitor activity in plants. *Int. J. Biol. Macromol.*, **178**: 253-262.

Wei L, Lu J, Xu H, Patel A, Chen Z-S, Chen G, 2015. Silver nanoparticles: synthesis, properties, and therapeutic applications. *Drug Discov. Today*, **20**: 595-601.

Zangeneh MM, Najafi F, Tahvilian R, Zangeneh A, Moradi R, 2017. Assessment of in vitro antibacterial properties of the hydroalcoholic extract of *Scrophularia striata* against *Staphylococcus aureus* (ATCC No. 25923)**.** *Int. J. Pharmacogn. Phytochem. Res*, **9**: 40-44.

Zhang H, Jacob JA, Jiang Z, Xu S, Sun K, Zhong Z, 2019. Hepatoprotective effect of silver nanoparticles synthesized using aqueous leaf extract of *Rhizophora apiculata*. *Int. J. Nanomed.*, **14**: 3517-3524.